J|A|C|S
ARTICLES
Published on Web 12/23/2006

Interactions of 1-Methylimidazole with $UO_2(CH_3CO_2)_2$ and $UO_2(NO_3)_2$: Structural, Spectroscopic, and Theoretical Evidence for Imidazole Binding to the Uranyl Ion

Keith E. Gutowski, Violina A. Cocalia, Scott T. Griffin, Nicholas J. Bridges, David A. Dixon,* and Robin D. Rogers*

Contribution from the Department of Chemistry and Center for Green Manufacturing, The University of Alabama, Shelby Hall, Box 870336, Tuscaloosa, Alabama 35487-0336

Received July 6, 2006; E-mail: dadixon@bama.ua.edu; rdrogers@bama.ua.edu

Abstract: The first definitive high-resolution single-crystal X-ray structure for the coordination of the 1-methylimidazole (Meimid) ligand to $UO_2(Ac)_2$ (Ac = CH_3CO_2) is reported. The crystal structure evidence is confirmed by IR, Raman, and UV−vis spectroscopic data. Direct participation of the nitrogen atom of the Meimid ligand in binding to the uranium center is confirmed. Structural analysis at the DFT (B3LYP) level of theory showed a conformational difference of the Meimid ligand in the free gas-phase complex versus the solid state due to small energetic differences and crystal packing effects. Energetic analysis at the MP2 level in the gas phase supported stronger Meimid binding over H_2O binding to both $UO_2(Ac)_2$ and $UO_2(NO_3)_2$. In addition, self-consistent reaction field COSMO calculations were used to assess the aqueous phase energetics of combination and displacement reactions involving H_2O and Meimid ligands to UO_2R_2 (R = Ac, NO_3). For both $UO_2(NO_3)_2$ and $UO_2(Ac)_2$, the displacement of H_2O by Meimid was predicted to be energetically favorable, consistent with experimental results that suggest Meimid may bind uranyl at physiological pH. Also, $\log(K_{nitrate}/K_{Ac})$ calculations supported experimental evidence that the binding stoichiometry of the Meimid ligand is dependent upon the nature of the reactant uranyl complex. These results clearly demonstrate that imidazole binds to uranyl and suggest that binding of histidine residues to uranyl could occur under normal biological conditions.

Introduction

The ability of imidazole and its derivatives to serve as coordinating ligands to uranyl (UO_2^{2+}) is of great interest as a model for understanding the interactions of biomolecules with uranium species, particularly for binding at histidine residues in proteins.[1] In a protein, histidine contains only one site that could bind to uranyl ions, the pyridine-like nitrogen atom from the imidazole moiety, and there is some evidence for this.[2,3] It is unlikely that binding occurs through the pyrrole-like NH group.[1] The predominant chemical form in which uranium will exist in physiological systems is the linear uranyl dication, which is ubiquitous under oxic conditions, with ligand binding occurring in the equatorial region.

There is relatively little known about the molecular interactions involved in the mechanism of uranyl transport and chemical toxicity in vivo. Uranium species can be transported in the blood via associations with blood plasma proteins or red blood cells[4] as uranyl−carbonate complexes and uranyl−protein−carbonate complexes.[5] Studies indicate that U(VI) can form strong complexes with blood transferrins, human albumin proteins, erythrocytes (red blood cells), and other low molecular mass species.[4,6] The metal ion binding site of transferrin proteins is comprised of an oxygen atom from an asparate residue, oxygen atoms from two deprotonated tyrosine residues, and nitrogen from a histidine residue. Serum albumins also play a role in metal ion transport, and some have a nitrogen atom from a histidine residue at the binding site.[7] Thus, a detailed understanding of the structural and electronic interactions of the histidine residue with uranyl is an important element in developing a better picture of the interactions of uranyl with proteins.

Most uranyl−amino acid crystal structures in the Protein Databank (PDB) consist of acidic amino acid complexes, usually with the free carboxylate terminus binding to uranyl.[8] This most common binding mode is via monodentate and/or bidentate chelation at uranium through the carboxylate oxygen atoms, which tend to form strong bonds with the uranyl cation,[9,10] just

(1) Sundberg, R. J.; Martin, R. B. *Chem. Rev.* **1974**, *74*, 471. Durbin, P. K. In *The Chemistry of the Actinide and Transactinide Elements*, 3rd ed.; Morss, L. R., Edelstein, N., Fuger, J., Eds.; Springer: Berlin, 2006; Chapter 31.
(2) Li, N. C.; Doody, E.; White, J. M. *J. Am. Chem. Soc.* **1957**, *79*, 5859.
(3) Levdikov, V. M.; Blagova, E. V.; Brannigan, J. A.; Cladière, L.; Antson, A. A.; Isupov, M. N.; Séror, S. J.; Wilkinson, A. J. *J. Mol. Biol.* **2004**, *340*, 767.
(4) Taylor, D. M. *J. Alloys Compd.* **1998**, *271*−*273*, 6.
(5) Huang, H.; Chaudhary, S.; Van Horn, J. D. *Inorg. Chem.* **2005**, *44*, 813.
(6) (a) Den Auwer, C.; Llorens, I.; Moisy, P.; Vidaud, C.; Goudard, F.; Barbot, C.; Solari, P. L.; Funke, H. *Radiochim. Acta* **2005**, *93*, 699. (b) Stevens, W.; Bruenger, F. W.; Atherton, D. R.; Smith, J. M.; Taylor, G. N. *Radiat. Res.* **1980**, *83*, 109.
(7) Bal, W.; Christodoulou, J.; Sadler, P. J.; Tucker, A. *J. Inorg. Biochem.* **1998**, *70*, 33.
(8) Van Horn, J. D.; Huang, H. *Coord. Chem. Rev.* **2006**, *250*, 765
(9) Alcock, N. W.; Flanders, D. J.; Kemp, T. J.; Shand, M. A. *J. Chem. Soc., Dalton. Trans.* **1985**, 517.
(10) Keramidas, A. D.; Rikkou, M. P.; Drouza, C.; Raptopoulou, C. P.; Terzis, A.; Pashalidis, I. *Radiochim. Acta* **2002**, *90*, 549.

10.1021/ja064592i CCC: $37.00

as found in inorganic carboxylate structures.[11] Coordination to a secondary amine has also been observed in iminodiacetate complexes with uranyl.[12]

A recent review of the literature of imidazole-based moieties in actinide-containing crystalline lattices as studied by X-ray diffraction concluded that most of the structures are based on imidazolium cations as outer sphere ligands, which do not directly interact with the uranium.[13] Perry et al.[14] reported that an X-ray crystal structure was refined to contain a $UO_2(NO_3)_2$ dimer bridged by two water molecules, although the hydrogen positions were never identified. It was suggested that two neutral 1H-imidazole molecules were present in the unit cell as outer sphere ligands. On the basis of infrared and X-ray photoelectron spectroscopy, it was subsequently concluded that the original structure was incorrect and that the structure actually is a hydroxide bridged dimer with two non-coordinating, 1,3-H-imidazolium cations in the outer sphere.[15]

Evidence for the direct involvement of imidazole and imidazole-based moieties in bonding in uranyl-containing complexes is less common. An ion exchange experiment showed that a histidine ligand can coordinate to the uranyl ion through the pyridine-like nitrogen from the imidazole moiety.[2] A uranyl−polypeptide low-resolution X-ray structure shows an imidazole coordinated to U with a U−N distance of 2.57 Å.[3] Other experiments including NMR,[16] calorimetry,[17] conductivity, and infrared (IR)[18] of imidazole-containing ligands to uranium suggest that coordination through the nitrogen atom is likely to be an important binding mode under biological conditions. The binding stoichiometries and complexation modes of the uranyl cation depended on the type of uranyl salt. Marzotto et al. crystallized solid samples of imidazole-containing complexes of $UO_2(CH_3CO_2)_2$ and $UO_2(NO_3)_2$ from ethyl acetate.[18] On the basis of IR assignments, they concluded that the nitrate complex consisted of two bound imidazole ligands (through the N atoms) and a bidentate and monodentate nitrate. The acetate complex contained a bidentate acetate, a bound water molecule, and a bound imidazolate anion, resulting in infinite chains, as in similar Co(II) and Zn(II) complexes.[19] However, the basic conditions used to prepare the transition metal complexes were not used in the preparation of the uranyl complexes, making the existence of the imidazolate questionable in the latter. ^1H and ^{13}C NMR studies of imidazole and 1-methylimidazole interactions with uranyl acetate and nitrate by Marzotto and Kozłowski[16] in aqueous solution and methanol showed that the use of water as a solvent resulted in no direct coordination of the imidazole moiety to the uranyl. This was attributed to the use of low pH in the range of 3−4, which results in protonation and formation of imidazolium species under these conditions. In methanol, the use of $UO_2(NO_3)_2$ yielded a 2:1 uranyl:ligand complex with both imidazole or 1-methylimidazole, whereas the use of $UO_2(CH_3CO_2)_2$ yielded 1:1 uranyl:ligand complexes.[16] The differing modes of complexation were similar to what was observed on the basis of IR measurements.[18] It was concluded that direct coordination of 1-methylimidazole would be likely to occur under physiological conditions where the low pH problem is not an issue and led to hypotheses for uranyl binding to histidine residues in proteins.[16] The NMR analysis was supported by a calorimetric study based on the higher heat for formation of the 1:2 $UO_2(NO_3)_2$:imidazole complex in solution versus the 1:1 $UO_2(CH_3CO_2)_2$:imidazole complex.[17]

Quantum chemical studies of actinide ions in both the gas phase and the solution phase have provided insight into properties that are difficult to measure experimentally, such as binding modes and condensed phase thermodynamics.[20] Quantum mechanical and molecular dynamics studies of uranyl:ligand systems with oxygen donors are by far the most common, including those with water,[21,22] acetate,[23,24] carbonate,[23,25] nitrate,[23,26] sulfate,[27] hydroxide,[28] and crown ethers.[29] Computational studies with nitrogen donors are few in number, paralleling the dominance of oxygen donor ligands in experimental studies. One of the few computational examples is a study of the uranyl porphyrin complex.[30] In addition, quantum chemical calculations coupled with continuum dielectric approaches[31] have been used to predict the solution structure and behavior of a range of metal cations, including alkali,[32] alkaline earth,[33] transition metal,[32−34] and f-element cations.[22,35]

We report here experimental results from single-crystal X-ray diffraction and optical spectroscopy for a neutral, mixed-donor UO_2^{2+}/1-methylimidazole complex, $UO_2(Ac)_2(Meimid)_2$ (Ac =

(11) Allen, P. G.; Bucher, J. J.; Clark, D. L.; Edelstein, N. M.; Ekberg, S. A.; Gohdes, J. W.; Hudson, E. A.; Kaltsoyannis, N.; Lukens, W. W.; Neu, M. P.; Palmer, P. D.; Reich, T.; Shuh, D. K.; Tait, C. D.; Zwick, B. D. *Inorg. Chem.* **1995**, *34*, 4797.
(12) Jiang, J.; Sarsfield, M. J.; Renshaw, J. C.; Livens, F. R.; Collison, D.; Charnock, J. M.; Helliwell M.; Eccles, H. *Inorg. Chem.* **2002**, *41*, 2799.
(13) Cocalia, V. A.; Gutowski, K. E.; Rogers, R. D. *Coord. Chem. Rev.* **2006**, *250*, 755.
(14) Perry, D. L.; Ruben, H.; Templeton, D. H.; Zalkin, A. *Inorg. Chem.* **1980**, *19*, 1067.
(15) Perry, D. L. *Inorg. Chim. Acta* **1982**, *65*, L211.
(16) Marzotto, A.; Kozłowski, H. *Inorg. Chim. Acta* **1982**, *67*, 87.
(17) Dawidowicz-Rozniatowska, J.; Kakołowicz, W.; Kozłowski, H. *Inorg. Chim. Acta* **1984**, *81*, L3.
(18) Marzotto, A.; Nicolini, M.; Braga, F.; Pinto, G. *Inorg. Chim. Acta* **1979**, *34*, L295.
(19) Eilbeck, W. J.; Holmes, F.; Underhill, A. E. *J. Chem. Soc. A* **1967**, 757.
(20) (a) Kaltsoyannis, N. *Chem. Soc. Rev.* **2003**, *32*, 9. (b) Schreckenbach, G.; Hay, J. P.; Martin, R. L. *J. Comput. Chem.* **1999**, *20*, 70. (c) Hay, P. J.; Martin, M. L. *Los Alamos Sci.* **2000**, *26*, 382.
(21) (a) Spencer, S.; Gagliardi, L.; Handy, N. C.; Ioannou, A. G.; Skylaris, C.-K.; Willetts, A.; Simper, A. M. *J. Phys. Chem. A* **1999**, *103*, 1831. (b) Hay, P. J.; Martin, R. L.; Schreckenbach, G. *J. Phys. Chem. A* **2000**, *104*, 6259. (c) Tsushima, S.; Suzuki, A. *J. Mol. Struct. (THEOCHEM)* **2000**, *529*, 21. (d) Tsushima, S.; Yang, T.; Suzuki, A. *Chem. Phys. Lett.* **2001**, *334*, 365. (e) Fuchs, M. S. K.; Shor, A. M.; Rösch, N. *Int. J. Quantum Chem.* **2002**, *86*, 487. (f) Hagberg, D.; Karlström, G.; Roos, B. O.; Gagliardi, L. *J. Am. Chem. Soc.* **2005**, *127*, 14250. (g) Bühl, M.; Diss, R.; Wipff, G. *J. Am. Chem. Soc.* **2005**, *127*, 13506. (h) Moskaleva, L. V.; Kruger, S.; Spörl, A.; Rösch, N. *Inorg. Chem.* **2004**, *43*, 4080. (i) Cao, Z.; Balasubramanian, K. *J. Chem. Phys.* **2005**, *123*, 114309. (j) Shamov, G. A.; Schreckenbach, G. *J. Phys. Chem. A* **2005**, *109*, 10961.
(22) Gutowski, K. E.; Dixon, D. A. *J. Phys. Chem. A* **2006**, *110*, 8840.
(23) de Jong, W. A.; Aprà, E.; Windus, T. L.; Nichols, J. A.; Harrison, R. J.; Gutowski, K. E.; Dixon, D. A. *J. Phys. Chem. A* **2005**, *109*, 11568.
(24) Vazquez, J.; Bo, C.; Poblet, J. M.; de Pablo, J.; Bruno, J. *Inorg. Chem.* **2003**, *42*, 6136.
(25) Gagliardi, L.; Grenthe, I.; Roos, B. O. *Inorg. Chem.* **2001**, *40*, 2976.
(26) Bühl, M.; Kabrede, H.; Diss, R.; Wipff, G. *J. Am. Chem. Soc.* **2006**, *128*, 6357.
(27) Craw, J. S.; Vincent, M. A.; Hillier, I. H.; Wallwork, A. L. *J. Phys. Chem.* **1995**, *99*, 10181.
(28) Hratchian, H. P.; Sonnenberg, J. L.; Hay, P. J.; Martin, R. L.; Bursten, B. E.; Schlegel, H. B. *J. Phys. Chem. A* **2005**, *109*, 8579.
(29) Guilbaud, P.; Wipff, G. *J. Phys. Chem.* **1993**, *97*, 5685.
(30) Liao, M.-S.; Kar, T.; Scheiner, S. *J. Phys. Chem. A* **2004**, *108*, 3056.
(31) Tomasi, J.; Mennucci, B.; Cammi, R. *Chem. Rev.* **2005**, *105*, 2999.
(32) (a) Asthagiri, D.; Pratt, L. R.; Paulaitis, M. E.; Rempe, S. B. *J. Am. Chem. Soc.* **2004**, *126*, 1285. (b) Westphal, E.; Pliego, J. R., Jr. *J. Chem. Phys.* **2005**, *123*, 074508-1.
(33) (a) Pavlov, M.; Siegbahn, P. E. M.; Sandström, M. *J. Phys. Chem. A* **1998**, *102*, 219. (b) Marcos, E. S.; Pappalardo, R. R.; Rinaldi, D. *J. Phys. Chem.* **1991**, *95*, 8928. (c) Asthagiri, D.; Pratt, L. R. *Chem. Phys. Lett.* **2003**, *371*, 613. (d) Katz, A. K.; Glusker, J. P.; Beebe, S. A.; Bock, C. W. *J. Am. Chem. Soc.* **1996**, *118*, 5752.
(34) Martínez, J. M.; Pappalardo, R. R.; Marcos, E. S. *J. Phys. Chem. A* **1997**, *101*, 4444.
(35) Cosentino, U.; Villa, A.; Pitea, D.; Moro, G.; Barone, V. *J. Phys. Chem. B* **2000**, *104*, 8001.

CH_3CO_2, Meimid = 1-methylimidazole), synthesized and crystallized in the ionic liquid (IL), 1-butyl-3-methylimidazolium chloride. A computational investigation was also undertaken to study the structural and energetic properties of the binding of water and Meimid molecules to both $UO_2(Ac)_2$ and $UO_2(NO_3)_2$ in the gas phase and in solution. These results clearly demonstrate that imidazole binds to uranyl and suggest that binding of histidine residues to uranyl could occur under physiological conditions.

Experimental Section

Sample Preparation. $UO_2(Ac)_2(H_2O)_2$ was obtained from Alfa Aesar, Ward Hill, MA, and used as received. Meimid was purchased from Aldrich Chemicals, Milwaukee, WI, and distilled prior to use. All other chemicals were of reagent grade, obtained from Aldrich, and used without further purification. The IL, 1-butyl-3-methylimidazolium chloride ([C_4mim]Cl), was synthesized by combining equimolar amounts of Meimid and *n*-butyl chloride in a round-bottom flask with moderate stirring and heating (70 °C) for 72 h following previous literature procedures.[36]

$UO_2(Ac)_2(Meimid)_2$ was first isolated from an impure IL containing excess, unreacted (i.e., incomplete alkylation) 1-methylimidazole to which solid $UO_2(Ac)_2(H_2O)_2$ had been added. The complex crystallized from the IL after heating to 60 °C followed by slow cooling to 34−35 °C. Whereas impurities such as water and chloride ion are often recognized as problems in using ILs, the presence of trace to high quantities of unreacted Meimid is often not examined. This has implications as unreacted Meimid may be a potential interferant in spectroscopic measurements, for example, of metal ions dissolved in ILs.

Once the new complex was isolated, a rational, reproducible synthesis was carried out taking advantage of the unique solvating properties of the IL.[37−39] Nine millimoles of $UO_2(Ac)_2(H_2O)_2$ was added to a solution of 37% (w/w) Meimid (0.05 mol) in pure [C_4mim]Cl followed by heating to 60 °C. Upon slow cooling to 34−35 °C, yellow crystals of the desired product precipitated directly from the IL. The crystals were filtered, collected, and washed with hexane. Single-crystal X-ray diffraction analysis (identical unit cell parameters) confirmed the product from the rational synthesis to be identical to the original compound.

Infrared Spectroscopy. 0.06 g of $UO_2(Ac)_2(Meimid)_2$ was dissolved in 0.5 g of acetonitrile, a drop of the solution was layered onto a polyethylene IR card, and the solvent was allowed to evaporate. Transmission spectra (Nicolette Magna-IR 560 FT-IR) were taken together with a background for 100 scans and processed with Omnic software.

Raman Spectroscopy. 0.06 g of $UO_2(Ac)_2(Meimid)_2$ was washed with hexane to eliminate any impurities, and, after drying, the solid was placed in an NMR tube that was later used for Raman measurements (utilizing a Jobin-Yvon HR800 UV confocal microscope). The excitation line of 632.81 nm is from a HeNe laser with approximately 12 mW of power at the sample. The shifts were detected using a Peltier cooled CCD detector.

UV−Vis Spectroscopy. A solution of 0.03 M $UO_2(Ac)_2(Meimid)_2$ or 2 mM $UO_2(Ac)_2(H_2O)_2$ dissolved in acetonitrile was placed in a 1.00 cm path length cuvette. Spectra were measured on a Varian Optical Cary 3C UV−visible spectrometer. Prior to recording the spectra, a baseline of the solvent (acetonitrile) was measured and automatically subtracted from each spectrum.

Single-Crystal X-ray Crystallography. The data were collected on a Bruker SMART diffractometer with a CCD area detector using graphite monochromated Mo Kα ($\lambda = 0.71073$ Å) radiation. A single crystal was mounted on a glass fiber and transferred to the goniometer for data collection. The crystal was cooled to −100 °C under a cold nitrogen gas stream. The structure was solved using the SHELXTL software package,[40] and the absorption corrections were made with SADABS.[41] The structure was refined by full-matrix least-squares on F^2. All of the non-hydrogen atoms were readily located, and their positions were refined anisotropically. Hydrogen atoms were also easily located and refined isotropically.

Computational Methods. The $UO_2(Ac)_2(R)_n$ and $UO_2(NO_3)_2(R)_n$ ($n = 1$ and 2) complexes with R = H_2O and/or Meimid were optimized using gradient-corrected density functional theory (DFT) with the hybrid B3LYP exchange-correlation functional.[42] All of our DFT geometry optimizations and frequency calculations were done with the Stuttgart 60 e small core RECPs and the corresponding Stuttgart orbital basis sets for the U atom[43] and the TZVP DFT-optimized orbital basis set for the O, N, C, and H atoms[44] following our prior work on uranyl complexes.[23] We eliminated the most diffuse functions in the U basis set, those with an exponent of 0.005 due to the difficulty in converging the wave function with such diffuse functions. These diffuse functions were replaced with diffuse functions with exponents of 0.013, 0.059, 0.026, and 0.067 for the s, p, d, and f functions, respectively, obtained by geometric extrapolation following our previous work.[22] Vibrational analysis was performed to ensure that each structure was a minimum on the potential energy surface.

Single-point MP2 calculations[45] at the optimized DFT geometries were also performed for all of the complexes with the modified Stuttgart small core basis set on uranium (with added g functions) and corresponding ECP and the aug-cc-pVTZ basis set[46] on the light atoms. We have shown previously that no significant BSSE effects are present by expanding the size of the basis set.[22,23] MP2 calculations were performed with the 1s core orbitals frozen on the light atoms and the 5s, 5p, and 5d orbitals frozen on uranium. Thermochemical corrections to the MP2 energies to obtain the free energies were made by using the geometries and frequencies obtained at the B3LYP/TZVP level.[47] Solvation effects were included at the COSMO (conductor-like screening model)[48] level using the Gaussian 03 implementation and a dielectric constant of 78.39 for bulk water. Natural bond orbital (NBO) analyses were performed at the optimized geometries at the B3LYP DFT level with the program Gaussian 03.[49]

All calculations were performed with the Gaussian 03[50] suite of programs on the SGI Altix 350 and Cray XD1 at the Alabama

(36) (a) Wilkes, J. S.; Lewiski, J. A.; Wilson, R. A.; Hussey, C. L. *Inorg. Chem.* **1982**, *21*, 1263. (b) Seddon, K. R.; Stark, A.; Torres, M. J. *Pure Appl. Chem.* **2000**, *72*, 2275.
(37) Visser, A. E.; Jensen, M. P.; Laszak, I.; Nash, K. L.; Choppin, G. R.; Rogers, R. D. *Inorg. Chem.* **2003**, *42*, 2197.
(38) (a) *Ionic Liquids in Synthesis*; Wasserscheid, P., Welton T., Eds.; VCH−Wiley: Weinheim, 2002. (b) *Ionic Liquids: Industrial Applications to Green Chemistry*; Rogers R. D., Seddon, K. R., Eds.; ACS Symposium Series 818; American Chemical Society: Washington, DC, 2002. (c) *Ionic Liquids as Green Solvents: Progress and Prospects*; Rogers, R. D., Seddon, K. R., Eds.; ACS Symposium Series 856; American Chemical Society: Washington, DC, 2003.
(39) (a) Welton, T. *Chem. Rev.* **1999**, *99*, 2071. (b) Holbrey, J. D.; Seddon, K. R. *Clean Prod. Proc.* **1999**, *1*, 223. (c) Wasserscheid, P.; Keim, W. *Angew. Chem., Int. Ed.* **2000**, *39*, 3772. (d) Sheldon, R. *Chem. Commun.* **2001**, 2399. (e) Gordon, C. M. *Appl. Catal., A* **2001**, *222*, 101. (f) Olivier-Bourbigou, H.; Magna, L. *J. Mol. Catal. A: Chem.* **2002**, *182−183*, 419. (g) Dupont, J.; de Souza, R. F.; Suarez, P. A. Z. *Chem. Rev.* **2002**, *102*, 3667.
(40) Sheldrick, G. M. *SHELXTL, version 6.14*; Bruker AXS, Inc.: Madison, WI, 2003.
(41) Sheldrick, G. M. *Program for Semiempirical Absorption Correction of Area Detector Data*; University of Göttingen: Germany, 1996.
(42) (a) Becke, A. D. *J. Chem. Phys.* **1993**, *98*, 5648. (b) Lee, C.; Yang, W.; Parr, R. G. *Phys. Rev. B* **1988**, *37*, 785.
(43) Küchle, W.; Dolg, M.; Stoll, H.; Preuss, H. *J. Chem. Phys.* **1994**, *100*, 7535; http://www.theochem.uni-stuttgart.de/.
(44) Godbout, N.; Salahub, D. R.; Andzelm, J.; Wimmer, E. *Can. J. Chem.* **1992**, *70*, 560.
(45) Møller, C.; Plesset, M. S. *Phys. Rev.* **1934**, *46*, 618.
(46) Dunning, T. H., Jr. *J. Chem. Phys.* **1989**, *90*, 1007.
(47) McQuarrie, D. A. *Statistical Mechanics*; University Science Books: Sausalito, CA, 2000.
(48) Klamt, A.; Schüürmann, G. *J. Chem. Soc., Perkin Trans. 2* **1993**, 799.
(49) (a) Reed, A. E.; Curtiss, L. A.; Weinhold, F. *Chem. Rev.* **1988**, *88*, 899. (b) Foster, J. P.; Weinhold, F. *J. Am. Chem. Soc.* **1980**, *102*, 7211. (c) Reed, A. E.; Weinhold, F. *J. Chem. Phys.* **1983**, *78*, 4066. (d) Reed, A. E.; Weinstock, R. B.; Weinhold, F. *J. Chem. Phys.* **1985**, *83*, 735. (e) Reed, A. E.; Weinhold, F. *J. Chem. Phys.* **1985**, *83*, 1736.

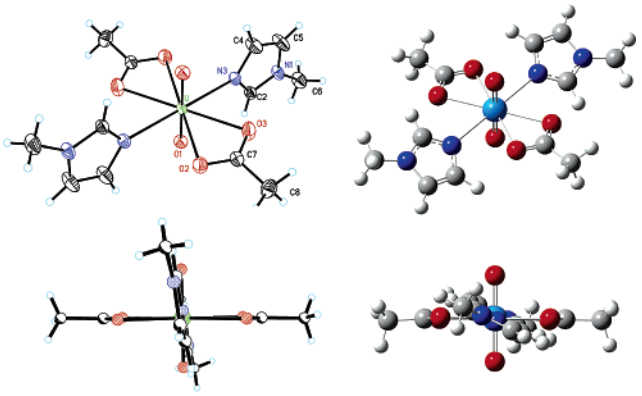

Figure 1. (Left) ORTEP (50% probability ellipsoids) diagram of $UO_2(Ac)_2(Meimid)_2$ showing hexagonal bipyramidal geometry about uranium, as well as side view (non-ORTEP). (Right) Optimized gas-phase structure of $UO_2(Ac)_2(Meimid)_2$ at the B3LYP/TZVP/Stuttgart level. Note the difference in the orientations of the Meimid groups.

Supercomputer Center, and the NWChem suite of programs[51] on the massively parallel 1980 processor HP Linux cluster in the Molecular Science Computing Facility in the William R. Wiley Environmental Molecular Sciences laboratory at the Pacific Northwest National Laboratory.

Results and Discussion

Crystal Structure. The crystal structure of $UO_2(Ac)_2(Meimid)_2$ (Figure 1) shows that the complex resides on a crystallographic inversion center with overall hexagonal bipyramidal geometry around the uranium center. The hexagonal plane of uranium (consisting of four oxygen and two nitrogen atoms) is planar to within 0.091 Å. The axial O═U═O fragment is collinear by symmetry with a $U{=}O_{ax}$ distance of 1.775(3) Å. The two trans acetate ligands are bidentate with nearly identical $U{-}O_{acetate}$ distances of 2.492(3) and 2.493(3) Å. The two trans Meimid molecules are coordinated through nitrogen with a unique U−N bond distance of 2.528(3) Å. Each heterocycle ring is oriented nearly perpendicular to the uranyl equatorial plane ($\delta = 83.4(3)°$), referenced to the dihedral angle $O_{ac}{-}U{-}N{=}C_2$. The uranium atom resides 0.204(9) Å out of each imidazole plane so that the two imidazole rings deviate from coplanarity with each other by 0.407(16) Å.

The $UO_2(Ac)_2(Meimid)_2$ complexes pack along the crystallographic *a* axis in the same orientation with alternating regions of Meimid and uranyl acetate along the *c* axis. There are two types of arrangements in the lattice. Down the *a* axis, the molecules form columns (Supporting Information), which consist of hydrogen-bonded "infinite one-dimensional chains". This is illustrated more explicitly in Figure 2, which shows that the hydrogen atom (H6A) from the methyl groups of Meimid interacts with the axial oxygen (O1) of uranyl from an adjacent $UO_2(Ac)_2(Meimid)_2$ molecule with an O···H close contact of ~2.6 Å indicative of a weak C−H···O═U hydrogen bond. The columns interact diagonally in the (*ab*) plane via acetate methyl hydrogen atom (H8A) and acetate oxygen (O3) short contacts. The adjacent columns along the *c* axis interact diagonally along the (*ac*) plane through short contacts between imidazole methyl hydrogen (H6B) and acetate oxygen (O2) atoms. These interactions are also illustrated in Figure 2.

$\pi-\pi$ interactions between the N1 atoms (3.690(7) Å) on the two imidazole rings oriented diagonally along the same (*ac*) plane may also be important in the crystal packing. The U−N bond distance (2.528(3) Å) is slightly shorter than the same distance in the $UO_2(NO_3)_2(Py)_2$ (2.543(13) Å)[52] (Py = pyridine) and $UO_2(Ac)_2$(4,4′-bipy) (2.636(7) Å) (4,4′-bipy = 4,4′-bipyridine) complexes.[53] This shows a stronger interaction between the metal center and the Meimid nitrogen, consistent with the higher basicity of Meimid ($pK_a = 7.20$)[54] as compared to Py ($pK_a = 5.23$)[55] and 4,4′-bipy ($pK_a = 4.82$).[56] This distance is also shorter than the same type of U−N interaction determined from a 1.6 Å resolution protein X-ray structure (2.57 Å),[3,8] with the advantage that our model offers not only the precision of a small molecule single-crystal structure determination, but also more structural information into the uranyl−imidazole interaction. The U═O, $U{-}O_{ac}$, $C{-}O_{ac}$, and $C{-}C_{ac}$ distances are consistent to within 0.01−0.02 Å with other hexagonal-bipyramidal uranyl−acetate complexes as determined by X-ray[57] and neutron[58] diffraction and EXAFS[59] solution studies.

Infrared, Raman, and UV−Vis Spectroscopy. Infrared and Raman spectroscopy have been extensively used to investigate the coordination modes of numerous uranyl compounds.[60,61] On the basis of a correlation between calculated and experimental results for a wide range of UO_2^{2+} stretching frequencies, the uranyl stretching frequencies (and the associated force constants) should decrease as the number of equatorial ligands to uranyl increases.[62] The (COO) stretching frequencies can be used to determine whether the binding mode of carboxylate anions are monodentate or bidentate.[23] Two frequencies have been previously reported for $\nu_s(O{=}U{=}O)$ in $UO_2(Ac)_2$: 852[63] and 841 cm^{-1}.[62] We find $\nu_s(O{=}U{=}O)$ at 840 cm^{-1} in the title compound from the Raman spectrum (Table 1 and Supporting Information), consistent with both values. Thus, the binding of Meimid does little to change the basic structure of the $UO_2(Ac)_2$ core. The IR spectrum (Table 1 and Supporting Information) shows an intense band at 916 cm^{-1} for the asymmetric uranyl stretch, close to the value of 928 cm^{-1} for $UO_2(Ac)_2$[62] and 910 cm^{-1} reported by Marzotto for the complex of uranyl acetate with imidazolate and water.[18] The IR data indicate that acetate binds as a bidentate ligand (with the symmetric ν_s(COO) and the

(50) Frisch, M. J.; et al. *Gaussian 03*, revision B.05; Gaussian, Inc.: Wallingford, CT, 2004.
(51) (a) Apra, E.; et al. *NWChem, Version 4.7*; William R. Wiley Environmental Molecular Sciences Laboratory, Pacific Northwest National Laboratory, Richland, WA, 2005. (b) Kendall, R. A.; et al. *Comput. Phys. Commun.* **2000**, *128*, 260.
(52) Pennington, M.; Alcock, N. W.; Flanders, D. J. *Acta. Crystallogr.* **1988**, *C44*, 1664.
(53) Alcock, N. W.; Flanders, D. J.; Brown, D. *Dalton Trans.* **1985**, 1001.
(54) Schoefield, K. *Hetero-aromatic Nitrogen Compounds*; Plenum Press: New York, 1967; p 146.
(55) *CRC Handbook of Chemistry and Physics*, 86th ed.; Lide, D. R., Ed.; CRC Press LLC: Boca Raton, FL, 2005−2006.
(56) Perrin, D. D. *Dissociation Constants of Organic Bases in Aqueous Solutions*; Butterworth: London, 1965.
(57) (a) Templeton, D. H.; Zalkin, A.; Ruben, H.; Templeton, L. K. *Acta Crystallogr.* **1985**, *C41*, 1439. (b) Zalkin, A.; Ruben, H.; Templeton, D. H. *Acta. Crystallogr., Sect. B* **1982**, *38*, 610. (c) Gutowski, K. E.; Bridges, N. J.; Rogers, R. D. In *The Chemistry of the Actinide and Transactinide Elements*, 3rd ed.; Morss, L. R., Edelstein, N., Fuger, J., Eds.; Springer: Berlin, 2006; Chapter 22.
(58) Navaza, A.; Charpin, P.; Vigner, D.; Heger, G. *Acta. Crystallogr., Sect. C* **1991**, *47*, 1842.
(59) (a) Denecke, M. A.; Reich, T.; Bubner, M.; Pompe, S.; Heise, K. H.; Nitsche, H.; Allen, P. G.; Bucher, J. J.; Edelstein, N. M.; Shuh, D. K. *J. Alloys Compd.* **1998**, *271−273*, 123. (b) Jiang, J.; Rao, L.; Di Bernardo, P.; Zanonato, P. L.; Bismondo, A. *J. Chem. Soc., Dalton Trans.* **2002**, 1832.
(60) Kakihana, M.; Nagumo, T.; Okamoto, M.; Kakihana, H. *J. Phys. Chem.* **1987**, *91*, 6128.
(61) Gal, M.; Goggin, P. L.; Mink, J. *J. Mol. Struct.* **1984**, *114*, 459.
(62) Quilès, F.; Burneau, A. *Vib. Spectrosc.* **1998**, *18*, 61.
(63) Nguyen-Trung, C.; Begun, G. M.; Palmer, D. A. *Inorg. Chem.* **1992**, *31*, 5280.

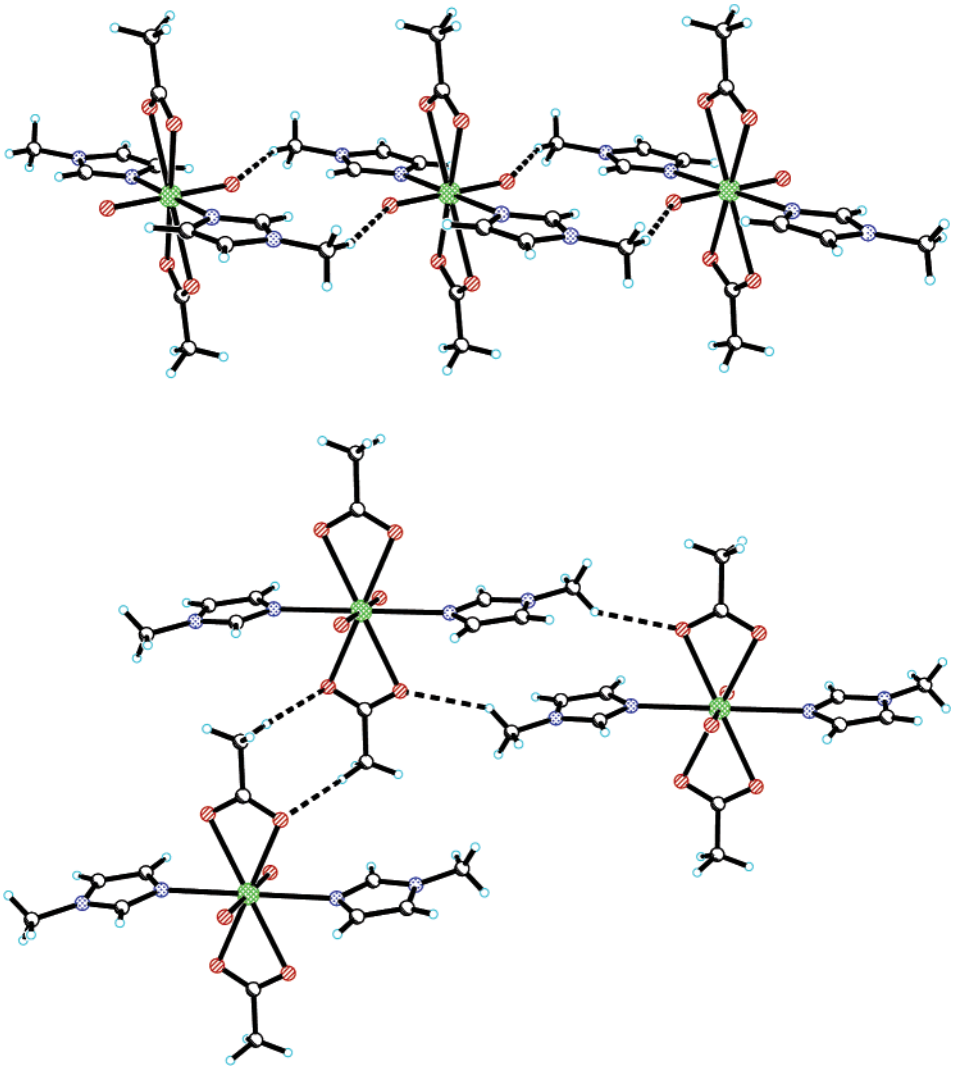

Figure 2. Crystallographic close contacts (dashed lines) between methyl (H)/O_{uranyl} and methyl (H)/$O_{acetate}$, illustrating infinite chains and diagonal interactions respectively.

Table 1. Geometric and Vibrational Frequency Comparison of X-ray and Predicted Gas-Phase Structures for $UO_2(Ac)_2(Meimid)_2$

parameter	experiment	gas phase I (C_1)	gas phase II (C_i)[a]
U═O (Å)	1.775(3)	1.774	1.783
U−$O_{acetate}$ (Å)	2.492(3)	2.521	2.513
U−$C_{acetate}$ (Å)	2.844(4)	2.911	2.900
U−$N_{imidazole}$ (Å)	2.528(3)	2.699	2.600
O−C−O (deg)	122.1(3)	119.3	119.5
O_{ac}−U−N═C_2 (deg)	83.4(3)[b]	23.0[b]	89.1[b]
$\nu_{sym}(UO_2^{2+})$ (cm^{-1})	840	893[c]	875[c]
$\nu_{asym}(UO_2^{2+})$ (cm^{-1})	916	975[d]	957[d]

[a] Second-order saddle point. [b] Due to the presence of the two rings, one of the dihedral angles is positive and the other is negative. [c] Calculated value in anhydrous $UO_2(CH_3CO_2)_2$: 906 cm^{-1}. [d] Calculated value in anhydrous $UO_2(CH_3CO_2)_2$: 990 cm^{-1}.

antisymmetric ν_a(COO) carboxylate stretching modes at 1468 and 1538 cm^{-1}, respectively) rather than a monodentate ligand, consistent with our previously calculated values for $UO_2(Ac)_2$.[23] The Raman measurements are also consistent (ν(CC) stretch at 955 cm^{-1}) with bidentate acetate binding to uranyl.[62]

The UV−vis spectra of $UO_2(Ac)_2(H_2O)_2$ and $UO_2(Ac)_2$-$(Meimid)_2$ dissolved in CH_3CN (Supporting Information) show no significant differences in peak shapes, suggesting equivalent coordination environments in both cases. Also, the visible absorption centered at 430 nm is consistent with other spectra for uranyl-containing complexes.[64]

Calculated Structures. The optimized gas-phase structures of Meimid and H_2O complexes with both $UO_2(Ac)_2$ and UO_2-$(NO_3)_2$ were calculated using DFT to study the energetics of ligand exchange following our previous study.[22] Table 2 contains the calculated geometric and vibrational parameters for the acetate and nitrate complexes with varying Meimid and H_2O compositions, including $UO_2(R)_2(H_2O)_n$, $UO_2(R)_2(Meimid)_n$, and $UO_2(R)_2(H_2O)(Meimid)$, where n = 0, 1, or 2 and R = CH_3CO_2 or NO_3. Binding of two acetate or nitrate ligands to the bare uranyl ion results in an elongation of the U═O bond by 0.068 and 0.059 Å, respectively, to 1.769 and 1.760 Å. This is consistent with more charge transfer in the acetate (0.76 e) complex versus the nitrate complex (0.73 e) and was also observed in a previous study using the local (SVWN) DFT method.[23]

The binding of one or two water molecules to these diacetate or dinitrate complexes results in a further increase in the U═O bond length, consistent with additional ligand-to-metal charge

(64) Feldman, I.; Koval, L. *Inorg. Chem.* **1963**, *2*, 145
(65) Dalley, N. K.; Mueller, M. H.; Simonsen, S. H. *Inorg. Chem.* **1971**, *10*, 323.

Table 2. Optimized B3LYP Geometric and Vibrational Parameters (Including NBO Uranyl Group Charges) for Uranyl Nitrate and Acetate Complexes with H_2O and Meimid Ligands

	NBO	bond distances (Å)				UO_2^{2+} str. (cm^{-1})	
complex	charge	U═O	U–O	U–OH_2	U–N_{Meimid}	ν_{sym}	ν_{asym}
UO_2^{2+}	+2.00	1.701				1041	1141
$UO_2(Ac)_2$	+1.24	1.769	2.394			906	990
$UO_2(Ac)_2(H_2O)$	+1.20	1.776	2.395[a]	2.537		894	977
			2.460[b]				
$UO_2(Ac)_2(H_2O)_2$	+1.15	1.774	2.478	2.561		894	977
$UO_2(Ac)_2(Meimid)$	+1.22	1.774	2.410[a]		2.564	895	978
			2.482[b]				
$UO_2(Ac)_2(Meimid)_2$	+1.19	1.774	2.521		2.699	893	975
$UO_2(Ac)_2(Meimid)(H_2O)$	+1.19	1.773	2.511	2.588	2.648	895	979
$UO_2(NO_3)_2$	+1.27	1.760	2.420			925	1011
$UO_2(NO_3)_2(H_2O)$	+1.22	1.767	2.425[a]	2.505		912	996
			2.461[b]				
$UO_2(NO_3)_2(H_2O)_2$	+1.16	1.768	2.484	2.552		910	995
$UO_2(NO_3)_2(Meimid)$	+1.20	1.772	2.443[a]		2.498	903	985
			2.477[b]				
$UO_2(NO_3)_2(Meimid)_2$	+1.14	1.773	2.525		2.596	895	978
$UO_2(NO_3)_2(Meimid)(H_2O)$	+1.16	1.770	2.509	2.583	2.566	903	987

[a] Distal to ligand, avg. [b] Proximal to ligand, avg.

transfer.[23] In the acetate mono- and di-aquo complexes, 0.80 and 0.85 e are transferred, respectively, with average U═O bond lengths of 1.776 and 1.774 Å. In the analogous nitrate complexes, 0.78 and 0.84 e are transferred, respectively, and the U═O bond lengths are 1.767 and 1.768 Å, slightly shorter than in the acetate complexes.

Interestingly, the U−OH_2 bond in the mono-aquo acetate complex is ~0.03 Å longer than that in the nitrate structure. This is due to a much closer O···H contact (between the acetate oxygen and water hydrogen) in the acetate complex (2.546 Å) than in the nitrate complex (3.361 Å), causing the U−OH_2 to elongate in the latter due to their distinctly different optimal structures (see the Supporting Information for structures). In the acetate complex, the water molecule is approximately in the equatorial plane (C_s symmetry), whereas in the nitrate, the water is perpendicular to this plane and rotated toward a single nitrate ligand (C_1 symmetry).

In the di-aquo complexes (Figure 3), the U−OH_2 bond lengths are nearly identical, at 2.561 and 2.552 Å, respectively, with comparably short O···H contacts in both cases (2.352 and 2.428 Å, respectively). In Table 3, we compare the experimental data for $UO_2(NO_3)_2(H_2O)_2$ obtained from neutron and X-ray diffraction with our computational results.[66−69] The average experimental (overall structures ± standard deviation) U═O, U−$O_{nitrate}$, and U−OH_2 bond distances are 1.742 ± 0.029, 2.501 ± 0.022, and 2.439 ± 0.026 Å, respectively. The calculated U═O and U−$O_{nitrate}$ (2.484 Å) distances are within the experimental error bars, but the average U−OH_2 distance is noticeably longer than the average experimental value by 0.113 Å. This is consistent with our previous donor−acceptor studies with water binding to the uranyl dication.[22] Inclusion of second sphere water molecules or a continuum solvation model rectifies this discrepancy leading to a shorter U−OH_2 bond.

The binding of the Meimid ligand to uranyl exhibits interesting characteristics with respect to rotation of the heterocyclic ring into and out of the equatorial plane of the uranyl. For example, the optimal $UO_2(Ac)_2$(Meimid) and $UO_2(NO_3)_2$-(Meimid) structures are markedly different (see the Supporting Information for structures) in this respect. In the acetate complex, two local minima were located, one with C_1 symmetry in which the plane of the imidazole ring was perpendicular to the uranyl axis, and one with C_s symmetry in which the ring was parallel to the uranyl axis. The C_1 structure was 0.9 kcal/mol lower in electronic energy than the C_s structure. In the nitrate complex, analogous C_1 and C_s structures were optimized, but the electronic energy of the C_s complex was 0.6 kcal/mol lower than that of the C_1 complex. This difference is consistent with the differences in the U−N_{imid} and O···H distances. The U−N_{imid} distance is 2.564 Å in the acetate and 2.498 Å in the nitrate. This difference of 0.07 Å is due to the steric repulsion

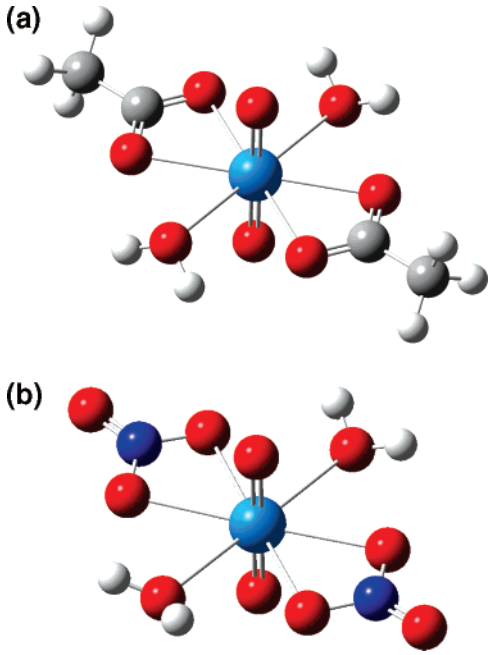

Figure 3. Optimized gas-phase structures of (a) $UO_2(Ac)_2(H_2O)_2$ and (b) $UO_2(NO_3)_2(H_2O)_2$ at the B3LYP/TZVP/Stuttgart level.

(66) Taylor, J. C.; Mueller, M. H. *Acta. Crystallogr.* **1965**, *19*, 536.
(67) Hughes, K.-A.; Burns, P. C. *Acta. Crystallogr., Sect. C* **2003**, *59*, i7.
(68) Shuvalov, R. R.; Burns, P. C. *Acta. Crystallogr., Sect. C* **2003**, *59*, i71.
(69) Eller, P. G.; Penneman, R. A. *Inorg. Chem.* **1976**, *15*, 2439.

Table 3. Geometric (Å, deg) Comparison of Experimental and Calculated Structures for $UO_2(NO_3)_2(H_2O)_2$

structure	U=O	U–$O_{nitrate}$	U–O_{H_2O}	O–N–O_{bound}
$UO_2(NO_3)_2(H_2O)_2$ (B3LYP)	1.768	2.484	2.552	113.6
$UO_2(NO_3)_2(H_2O)_2$ (neutron)[a]	1.754(4), 1.763(5)	2.513(5), 2.508(4), 2.491(5), 2.477(5)	2.457(4), 2.446(4)	115.3(3), 114.4(3)
$UO_2(NO_3)_2(H_2O)_2 \cdot 4H_2O$ (neutron)[b]	1.770(7), 1.749(7)	2.504(5), 2.547(6)	2.397(3)	114.6(5), 115.6(5)
$UO_2(NO_3)_2(H_2O)_2 \cdot H_2O$ (X-ray)[c]	1.738(6), 1.745(6)	2.490(7), 2.485(7), 2.539(6), 2.473(7)	2.453(6), 2.440(7)	117.1, 113.6
$UO_2(NO_3)_2(H_2O)_2 \cdot H_2O$ (X-ray)[d]	1.738(6), 1.778(6)	2.482(5), 2.494(4), 2.509(4), 2.516(4)	2.450(5), 2.481(4)	114.6, 113.9
$UO_2(NO_3)_2(H_2O)_2 \cdot 2H_2O \cdot 18C6$ (X-ray)[e]	1.693(6)	2.482(6), 2.486(6)	2.434(5)	114.7(7)

[a] From two crystallographically unique uranium sites, ref 65. [b] Reference 66. [c] From two crystallographically unique uranium sites, ref 67. [d] Reference 68. [e] Reference 69, 18C6 = 18-crown-6.

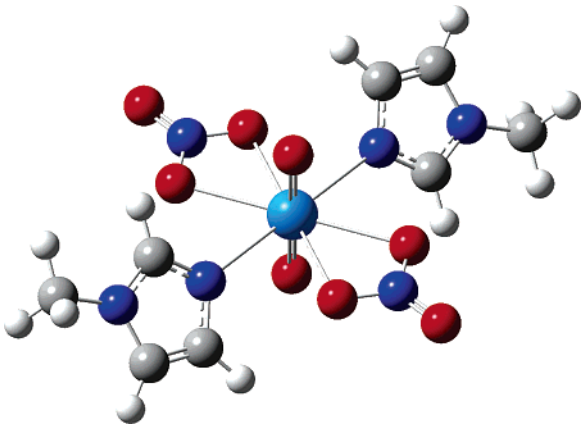

Figure 4. Optimized gas-phase structures of $UO_2(NO_3)_2(Meimid)_2$ at the B3LYP/TZVP/Stuttgart level.

encountered by the Meimid ligand in the equatorial plane due to interactions of the C2 and C4 ring hydrogen atoms with the acetate oxygen atoms (note the short O···H distances of 2.342 and 2.446 Å, respectively). In the nitrate complex, the orientation of the ring allows for a much stronger U−N interaction, and O···H contacts are not important in this case (>4 Å). This is also evident in the greater degree of charge transfer in $UO_2(NO_3)_2$(Meimid), and a considerably longer U=O bond length with respect to $UO_2(NO_3)_2$. However, the small energy differences at the B3LYP level for the C_1 and C_s structures in both the acetate and the nitrate complexes suggest that the barrier to rotation is very low and an average of both would be observed in solution. On the Gibbs free energy surface at 298 K, the C_s structure is favored in both cases, by 0.4 for the acetate complex and 1.2 kcal/mol for the nitrate complex.

Complexation of two Meimid ligands results in distinct similarities between the acetate and nitrate (Figures 1 and 4). Less charge transfer occurs as the imidazole ring rotates into the equatorial plane due to greater steric interactions between the ring hydrogen atoms and the acetate or nitrate oxygen atoms. In $UO_2(Ac)_2(Meimid)_2$, the $C_{2-}N-U-O_{Ac}$ dihedral angle is (±)23.0°, whereas in $UO_2(NO_3)_2(Meimid)_2$, the same angles are (±)44.6°, indicating that in the former complex, the rings are rotated to a greater extent away from the parallel uranyl axis and into the equatorial plane.

The difference in structure leads to differences in the NBO charges, U−N distances, and O···H contacts. Less charge transfer occurs in the acetate complex (0.81 e) versus the nitrate complex (0.86 e). The U−N bond distances are 2.699 and 2.596 Å, respectively, in the acetate and nitrate. The considerable lengthening of this bond in the acetate is due to two factors: strain and H-bonding. The greater O−C−O acetate bite angle induces more steric repulsion with the imidazole ligands, which pushes the rings away from the U.[23] Additionally, this larger angle allows for greater H-bonding to occur, thus causing the ring to rotate to maximize these interactions. The smaller O−N−O angle results in the same type of interactions, but to a lesser extent; O···H contacts in the acetate are 2.224 and 2.302 Å, and are noticeably longer in the nitrate, at 2.566 and 2.615 Å.

The calculated results can be compared to the crystal structure data in Table 1 and by comparing the structures shown in Figure 1. In the optimized B3LYP structure, the imidazole rings lie (±)23° out of the equatorial plane. In the solid-state crystal structure, the imidazole rings are nearly parallel to the uranyl axis, being (±)83.4(3)° out of the equatorial plane. A comparison of the X-ray structure and the optimized structure (gas phase I) reveals that the U=O and U−$O_{acetate}$ distances are in excellent agreement (0.001 and 0.029 Å, respectively). However, the calculated U−$N_{imidazole}$ distance is too long by 0.171 Å. This is due to the steric and H-bonding factors described above, which result in an elongation of the U−N bond when the ring approaches the equatorial plane.

A structure constrained with C_i symmetry (with the imidazole rings nearly parallel to the uranyl axis) was optimized at the same level of theory, and the results are given in Table 1 under gas phase II. This structure was a second-order saddle point, with the two imaginary frequencies (−21.0, −19.5 cm^{-1}) corresponding to a rotation of the rings toward the equatorial plane, and is 2.6 kcal/mol higher in energy. The U=O lengthens only slightly as compared to gas phase I (by 0.009 Å), but the U−$O_{acetate}$ and U−$N_{imidazole}$ bonds shorten and are now in better agreement with the experimental results differing from experiment by only 0.021 and 0.072 Å, respectively. The latter value is shortened by nearly 0.1 Å.

The differences in the experimental and gas-phase structures can be explained by considering the rotation barrier for the imidazole ring. At the B3LYP level, the electronic energy difference between structures I and II, corresponding to simultaneous rotation of both imidazole rings, is 2.6 kcal/mol. This small torsional barrier can easily be overcome in both solution and the solid state, especially if the rings do not rotate simultaneously. In the solid-state crystal structure, as shown in

Figure 2, a short contact exists between a methyl hydrogen atom (from Meimid) and a uranyl oxo ligand (~2.6 Å), as well as between a methyl hydrogen atom and an acetate oxygen atom (~2.6 Å). These weak interactions in the lattice could easily be responsible for the observed differences in the X-ray and isolated gas-phase structures, enabling the rotation barrier to be overcome by lattice packing interactions.

The geometries of mixed H_2O/Meimid uranyl acetate and nitrate complexes were also optimized to study ligand exchange energetics. The U═O, U−$O_{acetate}$, and U═$O_{nitrate}$ distances are nearly identical to the structures described above, which have hexagonal bipyramidal coordination around the uranium, with equal or slightly lower degrees of charge transfer. The U−OH_2 distances are ~0.03 Å greater than those in the analogous di-aquo complexes, probably due to the steric influence of the bulkier Meimid substituents.

In the acetate complex, the Meimid ligand is completely rotated into the equatorial plane ($C_{2-}N-U-O_{Ac} = 1°$), yet the U−N bond length is 0.05 Å shorter than in the lowest energy structure for the di-Meimid complex. In the mixed complex, the smaller H_2O ligand allows for less equatorial crowding, and the imidazole ring can more easily approach the U center. In the nitrate complex, the $C_{2-}N-U-O_{nitrate}$ dihedral angle is ±35°. The fact that the imidazole ring does not rotate entirely into the plane is due to a balance of factors between attaining a short U−N distance (2.566 Å) and ring rotation for H-bond stabilization. The O···H contacts in the acetates and nitrates are ~2.2 and ~2.4 Å, respectively. The structures for these complexes are given in the Supporting Information.

Calculated Vibrational Frequencies. Symmetric and asymmetric uranyl vibrational frequencies for all of the acetate and nitrate complexes are also listed in Table 2. Formation of the diacetate and dinitrate complexes from the bare uranyl ion results in a lowering of the symmetric stretch by 135 and 116 cm^{-1}, respectively, and the asymmetric stretch by 151 and 129 cm^{-1}, respectively, consistent with the amount of charge transfer to the uranium center and elongation of the U═O bond. This is also consistent with our previous work, which showed that this effect is more dramatic in the acetates than in the nitrates (for the mono-and di-ligand complexes).[23] In the acetates, formation of the H_2O and Meimid complexes results in lowering of the symmetric and asymmetric stretches by a value of ~12 cm^{-1} irrespective of the number of ligands.

The calculated uranyl symmetric and asymmetric stretches (Table 1) in structure gas phase I are 53 and 59 cm^{-1} higher than the experimental values. In structure gas phase II, these differences are reduced to 35 and 41 cm^{-1}, respectively, and the remaining differences will be due to neglect of anharmonic and long-range (second sphere) solvent effects as well as potential effects due to the functional that was used. This is consistent with earlier observations that binding of the ligand does little to affect the basic $UO_2(Ac)_2$ core.

For the nitrates, the degree of symmetric and asymmetric stretch lowering (with respect to $UO_2(NO_3)_2$) has a small dependence on the ligand. Formation of the mono- and di-aquo complexes results in a lowering of these stretches by 14 and 15 cm^{-1}, respectively. In the $UO_2(NO_3)_2$(Meimid) and mixed complexes, this lowering amounts to 22 and 25 cm^{-1}, respectively. Finally, in the $UO_2(NO_3)_2(Meimid)_2$ complex, the symmetric and asymmetric stretch lowering was 30 and 33 cm^{-1}, respectively. The calculated symmetric (910 cm^{-1}) and asymmetric (995 cm^{-1}) uranyl stretching frequencies for $UO_2(NO_3)_2(H_2O)_2$ are overestimated by ~35−55 cm^{-1} as compared to experiment[70] (ν_{sym} = 874 cm^{-1} and ν_{asym} = 948 cm^{-1} for $UO_2(NO_3)_2(H_2O)_2 \cdot 4H_2O$; ν_{sym} = 864 cm^{-1} and ν_{asym} = 941 cm^{-1} for $UO_2(NO_3)_2(H_2O)_2 \cdot H_2O$), consistent with the fact that the calculations are in the harmonic oscillator approximation as well as additional missing solvent effects and the use of an approximate exchange-correlation functional.

Calculated Energetics. A series of combination (A + B → AB) and displacement (AB + C → AC + B) reactions involving $UO_2(R)_2$ (R = Ac or NO_3) with H_2O and Meimid were investigated at the B3LYP and MP2 levels. The combination (1−6) and displacement (7 and 8) reactions that were studied for the uranyl acetates and nitrates are shown below.

$$UO_2(R)_2 + H_2O \rightarrow UO_2(R)_2(H_2O) \quad (1)$$

$$UO_2(R)_2(H_2O) + H_2O \rightarrow UO_2(R)_2(H_2O)_2 \quad (2)$$

$$UO_2(R)_2 + \text{Meimid} \rightarrow UO_2(R)_2(\text{Meimid}) \quad (3)$$

$$UO_2(R)_2(\text{Meimid}) + \text{Meimid} \rightarrow UO_2(R)_2(\text{Meimid})_2 \quad (4)$$

$$UO_2(R)_2(\text{Meimid}) + H_2O \rightarrow UO_2(R)_2(\text{Meimid})(H_2O) \quad (5)$$

$$UO_2(R)_2(H_2O) + \text{Meimid} \rightarrow UO_2(R)_2(\text{Meimid})(H_2O) \quad (6)$$

$$UO_2(R)_2(H_2O)_2 + \text{Meimid} \rightarrow UO_2(R)_2(H_2O)(\text{Meimid}) + H_2O \quad (7)$$

$$UO_2(R)_2(H_2O)(\text{Meimid}) + \text{Meimid} \rightarrow UO_2(R)_2(\text{Meimid})_2 + H_2O \quad (8)$$

The energy and enthalpy changes in the gas phase for reactions 1−8 for acetate and nitrate are provided in the Supporting Information, and the gas-phase free energy changes are in Table 4.

The B3LYP/TZVP/Stuttgart calculations were used to obtain the optimized structures, vibrations, and thermochemical corrections used in the higher-level MP2 calculations. We have shown previously that MP2 calculations involving large aug-cc-pVnZ (n = T or Q) basis sets for light atoms and the Stuttgart small core RECP and basis set (with g functions) on uranium in actinide-containing systems can adequately describe the binding energetics of the uranyl−water exchange reaction, and that BSSE corrections can be neglected.[22] The B3LYP results are consistently more positive than the MP2 results, between ~4 and 10 kcal/mol for the acetates and between ~4 and 12 kcal/mol for the nitrates, analogous to what was observed in our water binding study.[22] As a result, the B3LYP reaction energies, particularly the free energies, were not used for the solvation analysis and are included only for comparison.

The MP2 gas-phase reaction enthalpy change (ΔH_{298}) for the addition of a single water molecule to $UO_2(Ac)_2$ is quite negative (−21.4 kcal/mol). The positive entropy contribution resulting from the formation of a single molecule from two reactant

(70) McGlynn, S. P.; Smith, J. K.; Neely, W. C. *J. Chem. Phys.* **1961**, *35*, 105.

Table 4. Gas-Phase and Solution Reaction Free Energies (kcal/mol) in Aqueous Solution and Methanol for $UO_2(R)_2$ Complexes at 298 K[a]

rxn	ΔG_{gas}	ΔG_{soln} H_2O	log(*K*) H_2O	ΔG_{soln} MeOH	log(*K*) MeOH
		R = Ac			
(1)	−12.9	−13.4	9.8	−10.6	7.8
(2)	−6.9	−6.3	4.6	−3.5	2.6
(3)	−24.9	−20.7	15.2	−20.5	15.0
(4)	−7.7	−4.5	3.3	−4.0	2.9
(5)	−2.0	−1.2	0.9	1.7	−1.2
(6)	−14.0	−8.5	6.2	−8.2	6.0
(7)	−7.1	−2.2	1.6	−4.7	3.4
(8)	−5.7	−3.3	2.4	−5.7	4.2
		R = NO_3			
(1)	−17.4	−17.2	12.6	−14.1	10.3
(2)	−11.2	−9.5	7.0	−6.9	5.1
(3)	−34.0	−26.3	19.3	−26.1	19.1
(4)	−18.5	−15.6	11.4	−15.6	11.4
(5)	−8.5	−8.9	6.5	−6.1	4.5
(6)	−25.1	−17.9	13.1	−18.0	13.2
(7)	−13.9	−8.4	6.2	−11.1	8.1
(8)	−10.0	−6.7	4.9	−9.5	7.0

[a] Individual contributions to water and methanol solution energies provided in the Supporting Information.

molecules yields a ΔG_{298} of −12.9 kcal/mol. Addition of a second water is also very exothermic (ΔH_{298} = −17.7 kcal/mol), and the $-T\Delta S$ contribution (10.8 kcal/mol) is larger, making ΔG_{298} relatively less favorable at −6.9 kcal/mol. In this second reaction, the $-T\Delta S$ contribution is comparable to the gas-phase equivalent for a single free H_2O molecule of 13.5 kcal/mol. Thus, there is a minor entropy effect for the binding of a second H_2O molecule to $UO_2(Ac)_2$, and the only significant contribution is the loss of entropy of the free water molecule. Thus, $UO_2(Ac)_2(H_2O)$ and $UO_2(Ac)_2(H_2O)_2$ have comparable flexibility.

The addition of a single Meimid ligand to $UO_2(Ac)_2$ is considerably more exothermic than that of H_2O, with ΔH_{298} = −36.0 kcal/mol, a difference of 14.6 kcal/mol. This is a result of the higher Lewis basicity of the Meimid ligand as compared to H_2O, on the basis of the gas-phase proton affinities of 229.3 and 165.0 kcal/mol,[71] as well as H-bonding stabilizing effects, The $-T\Delta S$ contribution of 11.1 kcal/mol for this reaction is roughly one-half that of the calculated $-T\Delta S$ for the free Meimid ligand (22.2 kcal/mol), resulting in a reaction free energy of −24.9 kcal/mol. However, the addition of a second heterocyclic ligand is comparatively less exothermic, with a ΔH_{298} value of only −17.3 kcal/mol, primarily due to the steric factors described above in the geometric analysis, which lengthens the U−N bond (weakens the interaction). The $-T\Delta S$ contribution for this reaction is 9.6 kcal/mol, resulting in a reaction free energy of −7.7 kcal/mol. In the Meimid combination reactions (3 and 4), there is a relatively greater amount of conformational flexibility in the products as compared to the H_2O-containing products, as evidenced by the small $-T\Delta S$ contributions, which are comparable to the water reactions.

The remaining two combination reactions (5 and 6) involving the formation of mixed ligand complexes show distinctly different reaction energetics depending on the reactant ligand. The addition of an H_2O molecule to $UO_2(Ac)_2$(Meimid) is slightly favorable, with a reaction free energy of only −2.0 kcal/mol. However, the addition of Meimid to $UO_2(Ac)_2(H_2O)$ is quite favorable, with a reaction free energy of −14.0 kcal/mol. This is due to the higher Lewis basicity of the Meimid ligand and is consistent with what was observed for reactions 1−4. The $-T\Delta S$ contributions in these reactions are also consistent with previous results. The $-T\Delta S$ contribution (10 kcal/mol) for the water reactions approaches the gas-phase $-T\Delta S$ value for H_2O at 298 K, whereas the greater conformational flexibility of the Meimid product results in a $-T\Delta S$ contribution (12.7 kcal/mol) comparable to that of the water reaction.

The displacement reactions (7 and 8) are shown with respect to water displacement by the Meimid ligand. Understanding and accurately quantifying the energetics of these reactions in the gas phase is critical to assessing the solution-phase behavior. The free energy change of the first reaction, in which a bound H_2O molecule is displaced by a Meimid ligand from the diaquo complex, is −7.1 kcal/mol. Interestingly, the subsequent reaction, in which the remaining water molecule is displaced, is favorable by −5.7 kcal/mol, an amount comparable to the single water displacement. The free energy difference between the two reactions of only −1.4 kcal/mol is quite small and is consistent with what was found for the combination reactions. The small difference is attributable to the steric factors involved with binding a second Meimid ligand. The difference between ΔH_{298} and ΔG_{298} for these two reactions is +1.9 and −0.4 kcal/mol, respectively, indicating that the reaction energetics are dominated by the reaction enthalpy exothermicity, consistent with the fact that there is no net change in the number of free particles. If one compares ΔE_{elec} and ΔH_{298} for the reactions, there is no difference, meaning that the change in electronic energy is the driving force for the reaction.

The reaction energetics for the $UO_2(NO_3)_2$ complexes involving H_2O and Meimid are also listed in Table 4 and the Supporting Information. The individual reactions here warrant little additional discussion, as the conclusions are essentially the same as those found for the acetates. For all of the combination and displacement reactions studies, the reaction enthalpies and free energies are significantly negative, indicating that they are favored in the gas phase as was observed for the acetates. However, it is important to note that in all of the reactions, the free energy changes for the nitrates are significantly more negative than those for the acetates, in the range of −4.3 to −11.1 kcal/mol. The reason for this is due to the slightly greater electron-donating character of the acetate ligand to the uranyl over the nitrate ligand, thus allowing for a greater Lewis acid−base interaction with the H_2O and Meimid ligands in the nitrate complexes. The equatorial bulkiness of the nitrate is less than that of the acetate (indicated by a smaller bite angle and absence of methyl group), thus allowing equatorial Lewis base ligands to interact more strongly due to smaller steric constraints.

Quantum chemical continuum solvation models can be used to study the solution energetics of the binding of uranyl to imidazole and related compounds. The continuum-based solvation model used in this study partitions the solute−solvent environment into two distinct regimes, one of which is a cavity containing the solute molecule, and the other is the solvent medium surrounding the cavity defined solely by its dielectric constant. Induced charges on the surface of the cavity due to solute−solvent polarization allow one to obtain the free energy

(71) Hunter, L. P.; Lias, S. G. *J. Phys. Chem. Ref. Data* **1998**, *27*, 413.

of solution of the solute under study. To obtain solution energetics, accurate calculations in the gas phase are required as the solvation corrections are in addition to the gas-phase free energies.[31]

Table 4 contains the COSMO solvation free energy contributions to the solution free energy for the uranyl acetate and nitrate reactions 1−8 described previously. The solvation energy corrections, both electrostatic and nonelectrostatic (included separately in the Supporting Information), were applied to the MP2 gas-phase reaction free energies. The electrostatic contributions for nearly all of the reactions (except the final displacement reaction) are small, positive values. In the combination reactions, this is due to the differential solvation of two smaller reactant molecules over one larger product molecule. In the displacement reactions, the electrostatic solvation free energy contribution is very small, and in fact almost negligible, due to the stoichiometry of the reaction, in which the same number of particles is maintained on each side. The final displacement reaction for both the acetate and the nitrate has a negative electrostatic contribution to the solution free energy, likely due to better solvation of the smaller free H_2O molecule. It is important to note that in all of the reactions for the acetates and nitrates, the nonelectrostatic contribution to the solution free energy appears quite small, in the range of +1.1 to −2.0 kcal/mol. However, for some reactions, this contribution is actually a large percentage of the electrostatic energy and must be included for completeness. The total solvation contribution to the solution free energy is listed as ΔG_{solv}(total) in the Supporting Information. For all of the reactions, the total solvation contribution is positive, ranging from 0.0 to 7.4 kcal/mol for the acetates and 0.8 to 9.6 kcal/mol for the nitrates.

Also included in the Supporting Information is a standard state free energy correction ($\Delta G_{S.S.}$) needed to appropriately describe the aqueous solution chemistry. Summing ΔG_{gas} and ΔG_{solv}(total) yields the solution free energy change that is appropriate only for the hypothetical gas-phase concentration of 1 M at $P = 1$ atm and $T = 298.15$ K. If a different standard state is used, corresponding to solution concentrations of Meimid and H_2O of 1 M ($P = 24.5$ atm) and 55 M ($P = 1354$ atm), respectively, at 298.15 K, then the free energies must be adjusted accordingly.[72] In the combination reactions, where there are Meimid and H_2O molecules as free reactant entities, this amounts to a reduction in the reaction free energies of −1.9 and −4.3 kcal/mol, respectively. In the displacement reactions, the differential free energy adjustment due to the presence of H_2O products and Meimid reactants results in an adjustment in the reaction free energies by +2.4 kcal/mol.

The resulting corrected reaction free energies in aqueous solution, ΔG_{soln}, are also shown in Table 4. ΔG_{soln} is found to be negative for all of the acetate and nitrate combination and displacement reactions, indicating that the studied reactions should be spontaneous (favorable) in solution from a thermodynamic standpoint. For the acetate combination reactions, it is interesting to compare the free energy differences between reactions, $\delta\Delta G_{soln}$, in which Meimid and H_2O competitively bind to the same uranyl reactant complex. $\delta\Delta G_{soln}$ values defined as $\delta\Delta G = \Delta G(b) - \Delta G(a)$ (for (a,b)) for the reaction pairs (1,3), (2,6), and (5,4) for R = Ac are −7.3, −2.2, and −3.3 kcal/mol, respectively, with the reaction with Meimid being favored in each case.

In solution, although there may be competition between the ligands, the binding of Meimid is favorable in each case and will ultimately be the thermodynamic product. Log(K) values were calculated for the reactions using $\log K = -\Delta G_{soln}/(2.303RT)$. For the reactions pairs (1,3), (2,6), and (5,4) for R = Ac, the ratios of the $\log(K_b/K_a)$ values were determined to be 5.4, 1.6, and 2.4, respectively. Assuming that reaction pair (5,4) for R = Ac is the observed set of competing reactions in solution, it would be expected that the di-Meimid product would be the favored product over the mixed ligand complex in solution by a ratio of log(K) values of 2.4. The displacement reactions 7 and 8 for R = Ac for the substitution of H_2O by Meimid also favor the Meimid-substituted products, by −2.2 and −3.3 kcal/mol, for the single and double displacement reactions, respectively. Of course, $\log(K_7)$ and $\log(K_8)$ can be obtained from $\log(K_6/K_2)$ and $\log(K_3/K_1)$, respectively.

A comparison of the ΔG_{soln} values for the nitrate and acetate systems shows that the former are always more negative than the latter by −3.4 to −11.6 kcal/mol. The $\delta\Delta G_{soln}$ values for reaction pairs (1,3), (2,6), and (5,4) for R = NO_3 are −9.1, −8.4, and −6.7 kcal/mol, respectively, considerably more favorable than the analogous acetate reactions. Here, the $\log(K_b/K_a)$ equilibrium values are 6.7, 6.2, and 4.9, respectively.

It has been noted previously by both Marzotto and Kozłowski[16] and Dawidowicz-Rozniatowska[17] from experimental measurements, primarily in methanol, that uranyl acetate and uranyl nitrate exhibit differing coordination preferences for imidazole or 1-methylimidazole. It was observed that the 1:1 $UO_2(Ac)_2$:ligand and 1:2 $UO_2(NO_3)_2$:ligand complexes formed under otherwise similar conditions. These observations are directly supported by our solvation calculations. The reaction free energies in solution for reaction 3 for both R = Ac and NO_3 are both very exothermic, indicating that they are thermodynamically favorable in solution. However, reaction 4 for R = Ac is far less favorable than reaction 4 for R = NO_3 for the formation of the disubstituted Meimid acetate and nitrate complexes, respectively, by 11.1 kcal/mol. The $\log(K_{nitrate}/K_{Ac})$ value for this reaction is 8.1, suggesting that the $UO_2(NO_3)_2$-$(Meimid)_2$ complex would be distinctly favored in a solution containing both uranyl reactants. Displacement reaction 8 for both R = Ac and NO_3 forming the disubstituted Meimid complexes from a mixed ligand complex also shows the same trend. The reaction free energy in solution for reaction 8 for R = NO_3 is more negative than that of reaction 8 for R = Ac by 3.4 kcal/mol. In addition, the $\log(K_{nitrate}/K_{Ac})$ value for (8) is 2.5, suggesting the equilibrium preference for the disubstituted nitrate complex over the acetate complex.

These results suggest that Meimid will directly participate in binding to the uranyl cation in solution at neutral pH and will also displace water molecules in the first hydration sphere. This has implications for the complexation of the uranyl ion with histidine residues in proteins in biological systems. At physiological pH, it is highly likely that the nitrogen of the imidazole side chain in histidine may directly bind the uranyl cation, and the energetics of binding will be dependent upon the ligand substitution pattern around the uranyl. This is

(72) (a) Asthagiri, D.; Pratt, L. R.; Ashbaugh, H. S. *J. Chem. Phys.* **2003**, *119*, 2702. (b) Ben-Naim, A.; Marcus, Y. *J. Chem. Phys.* **1984**, *81*, 2016. (c) Marcus, Y. *Biophys. Chem.* **1994**, *51*, 111. (d) Hummer, G.; Pratt, L. R.; García, A. E. *J. Phys. Chem.* **1996**, *100*, 1206. (e) Martin, R. L.; Hay, P. J.; Pratt, L. R. *J. Phys. Chem. A* **1998**, *102*, 3565.

consistent with experimental studies in methanol, which have concluded that imidazole may be involved in UO_2^{2+} binding at histidine side chains in proteins under conditions in which the imidazole is not protonated and may play an important role in bioinorganic complexes.

Table 4 and the Supporting Information also contain COSMO results using a dielectric constant for that of methanol (MeOH) for reactions 1−8. The results observed for H_2O and MeOH solvents are very similar as the large magnitudes of the dielectric constants (78.39 for H_2O and 32.53 for MeOH)[73] result in nearly negligible differences in the electrostatic contributions. The largest differences between H_2O and MeOH are the individual nonelectrostatic contributions, which cancel in the reactions, similar to the reactions in water. Standard state corrections are affected by solvent choice in the cases of reactions 1, 2, 5, 7, and 8 due to different effective concentrations in solution. The experimental conclusions in MeOH are also likely to be true for H_2O, supporting the original hypotheses.[16,17]

Li et al. reported equilibrium constants for the binding of UO_2^{2+} (in the form of a chloride) to histidine and histidine methyl ester, obtained from ion exchange measurements.[2] They observed two different log(*K*) values of 7.72 and 5.76 for histidine and histidine methyl ester, respectively, and concluded that these corresponded to carboxylate and imidazole chelation, respectively. Their results suggest relatively tight binding of the histidine ethyl ester ligand to the uranyl, consistent with many of our calculated log(*K*) values, although lack of exact experimental details precludes a direct, quantitative comparison.

Conclusions

The single-crystal X-ray structure of $UO_2(Ac)_2(Meimid)_2$ has been solved, clearly showing the bonding of the nitrogen atom of Meimid to uranyl. Spectroscopic data, including IR, Raman, and UV−vis spectra, are fully consistent with the X-ray structure. This is the first high-resolution structural evidence for the coordination of the imidazole ring to the uranyl cation in the solid state. Electronic structure calculations on $UO_2(Ac)_2(Meimid)_2$ show differences between the free complex in the gas-phase and the solid-state structure. Because of a low rotational barrier of the Meimid ligand about the U−N bond in the gas phase, crystal packing effects (H-bonding) strongly influence the conformational preference of the Meimid ligand, resulting in slightly different ligand orientations. This suggests that, in solution, the Meimid ligand would likely undergo free rotation, sampling all conformations.

Calculations on $UO_2(Ac)_2$ and $UO_2(NO_3)_2$ complexes with Meimid and H_2O showed differences in complexation geometries and binding energetics as a function of ligand type. Ligand binding to $UO_2(NO_3)_2$ was always more exothermic than binding to $UO_2(Ac)_2$ due to charge transfer and steric effects. Self-consistent reaction field models (using the COSMO approach) have provided insights into solution-phase behavior, particularly with respect to H_2O/Meimid ligand exchange. Our calculations indicate that Meimid will displace H_2O molecules in the first coordination sphere of both $UO_2(Ac)_2$ and $UO_2(NO_3)_2$ complexes in the gas phase and in aqueous solution. The predicted $\log(K_{nitrate}/K_{Ac})$ ratios support the experimental evidence, which shows that the Meimid complexation stoichiometries depend on ligand type (Ac or NO_3). Also, Meimid complexation was more favorable than H_2O complexation due to differences in the Lewis basicity of the ligands.

Our results strongly suggest that Meimid will directly coordinate to the uranyl cation at pH's where the imidazole is not protonated, for example, at physiological pH. Thus, it is very likely that the imidazole moiety in histidine residues of proteins will directly coordinate to the uranyl cation. The actual energetics of binding will depend exactly on the environment of the ligands around the uranyl core. In addition to the biochemical implications, our results also suggest that unreacted Meimid can be a potential interferant in applications, for example, spectroscopic, involving metal ions dissolved in ILs.

Acknowledgment. This research was supported in part by the U.S. Department of Energy Environmental Management Science Program (Grant DE-FG02-05ER63989) and Division of Chemical Sciences, Geoscience, and Bioscience, Office of Basic Energy Sciences, Office of Science (Grant DE-FG02-96ER14673). Part of this work was supported by the U.S. Department of Energy, Office of Basic Energy Sciences, Geosciences Research Program. D.A.D. is indebted to the Robert Ramsay Endowment of the University of Alabama. This research was performed in part using the Molecular Science Computing Facility (MSCF) in the William R. Wiley Environmental Molecular Sciences Laboratory, a national scientific user facility sponsored by the U.S. Department of Energy's Office of Biological and Environmental Research and located at the Pacific Northwest National Laboratory, operated for the Department of Energy by Battelle. We would like to thank Dr. Shane Street and James Burgess from the University of Alabama Chemistry department for their assistance in acquiring IR and Raman spectra, funded under the Cooperative Agreement No. DE-FG02-01ER45867 titled "Alabama DOE/EPSCoR Program".

Supporting Information Available: Extended reference citations with complete author listings for refs 50 and 51. Crystal and refinement data for $UO_2(Ac)_2(Meimid)_2$ and crystallographic CIF file. Gas-phase B3LYP and MP2 energy, enthalpy, and free energy data and COSMO solvation contributions for reaction free energies in water and methanol. Additional crystal packing diagrams, Raman IR, and UV/vis spectra, and other remaining optimized structures. Cartesian coordinates for all species at the B3LYP/TZVP/Stuttgart level. This material is available free of charge via the Internet at http://pubs.acs.org.

JA064592I

(73) Gaussian 03 reference manual; http://www.gaussian.com/g_ur/k_scrf.htm.